

STUDIES OF THE ATMOSPHERIC WATER BALANCE

by

J. L. Rasmussen



Colorado Water

Resources Research Institute

Completion Report No. 24

Colorado
State
University

STUDIES OF THE ATMOSPHERIC WATER BALANCE

Completion Report

OWRR Project No. B-035-COLO

by

J. J. Rasmussen
D. L. Hadley
R. W. Furman
L. K. Balick

Department of Atmospheric Science
Colorado State University

submitted to
Office of Water Resources Research
U. S. Department of Interior
Washington, D.C. 20240

June 30, 1971

The work upon which this report is based was supported (in part) by funds provided by the United States Department of the Interior, Office of Water Resources Research, as authorized by the Water Resources Research Act of 1964, and pursuant to Grant Agreement No. 14-01-0001-1887

Colorado Water Resources Research Institute
Colorado State University
Fort Collins, Colorado

Norman A. Evans, Director

TABLE OF CONTENTS

STUDIES OF THE ATMOSPHERIC WATER BALANCE

	Page
Abstract	i
Part I: Atmospheric Water Balance and Annual Flow of the Upper Colorado River	1.
1. Introduction	1.
2. Procedures	3.
3. Results	6.
4. Conclusions and Recommendations	8.
Bibliography	10.
Part II: Atmospheric Water Balance and Precipitation Regimes of Extratropical Cyclones	12.
1. Introduction	12.
2. Analysis	13.
3. Conclusions	24.
Bibliography	30.

ABSTRACT

The atmospheric water balance computation is used for two distinctly different kinds of applications in this paper. First, the atmospheric water balance is used to infer the exchange of water at the earth's surface over the upper Colorado River Basin. Through the observation of the fluxes of water vapor over the basin and the observation of the changes with time of water stored in the atmosphere over the basin this exchange, precipitation minus evaporation, is determined. Thirteen winter seasons (1957-1969) were studied, twelve-hourly computations were accumulated from November 1, through April 30 and the resulting seasonal accumulation of water was correlated to the succeeding twelve months discharge from the basin. The results of this portion of the study, using the thirteen winter sample, are not encouraging. The correlation between runoff and accumulation is $r = 0.54$. This correlation is made up of two distinct chronologically ordered inputs. The first seven years show a remarkably good correlation $r = 0.82$. The final six years contain most of the scatter $r = 0.34$. Recent evidence of systematic errors in the measurement of humidity are presented as a possible cause of this deterioration in correlation between the computed precipitation minus evaporation and annual river discharge.

The second application of the water balance technique was centered on the study of the precipitation mechanisms within large extratropical cyclone storm systems. Here we show the circulation of mass and moisture within the storm system and demonstrate the relationship of this circulation to the production of precipitation. The ratio of precipitation rate to condensation rate is shown to be 0.90 for two storm cases. The condensation is shown to be largely formed at quite warm temperatures (warmer than -10°C). Finally a very localized intense band of precipitation is investigated and a hypothesis presented that suggests the localized precipitation extreme is related to the dynamic effects of a low level wind configuration initiating convective activity.

PART I

Atmospheric Water Balance and Annual Flow of the Upper Colorado River

1. Introduction

The ability to forecast river flow with a lead time of six to twelve months is becoming more and more important as the development of the water resource system increases. This is particularly true in the water resource conscious arid regions. The purpose of this paper is to summarize research into the possibility of using the atmospheric water balance technique to compute the water available for runoff from the Upper Colorado River Basin and to relate this to the actual runoff. The Upper Colorado derives most of its annual flow from the melt of snow in the alpine and forest zones of the Central Rocky Mountains; this built-in lag between the period of accumulation (November to April) and the succeeding twelve month runoff period (April to March) provides a desirable, if not optimum, forecast lead time.

The terrestrial water balance of a river basin may be written:

$$P - E = R_e + S_e \quad \text{I.1.1}$$

where P and E are the rates of precipitation and evapotranspiration over the area of the basin respectively. R_e is the rate of discharge of water from the basin, the runoff, and S_e is the change in storage of surface and ground water. The measurement of precipitation is difficult from both mechanical and sampling points of view (e.g. Weiss and Wilson, 1958; La Rue and Younkin, 1963). This difficulty increases when one seeks a representative precipitation estimate for a large mountain region (e.g. McDonald, 1960; Rasmussen, 1970a). Practically any textbook on applied

climatology addresses the problem of the difficulty in measuring evapo-transpiration and no really dependable computational technique is suitable for a large mountainous region. The aim of the research reported herein is to evaluate an alternative technique in the estimation of $P - E$ so that reliance upon the more difficult direct measurements and/or empirical methods are less critical. The analogous equation for the atmosphere's water balance is:

$$P - E = -R_a - S_a \quad 1.1.2$$

here the R_a is net outflow of water, ice and vapor from the atmospheric column above the basin and S_a is the change of storage of water, ice and vapor in the volume. Measurement of the right hand side of 1.1.2 provides the alternative scheme to estimation of the $P - E$ in the terrestrial water budget 1.1.1. The details of the atmospheric data availability and errors are discussed in the literature, for example Palmen (1967) or Rasmussen (1970a) and the reader is referred to these articles as well as a more specific paper, Rasmussen (1970b), pertaining to this research program.

The scheme outlined above is illustrated in the diagram of Figure 1 (Rasmussen (1970b)).

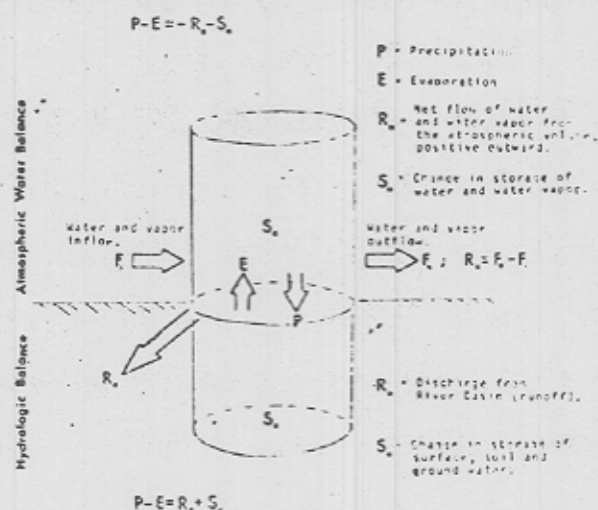


Figure 1. The atmospheric water balance and hydrologic balance. Dimensions are mass of water per unit time.

Our goal there is to measure the fluxes of water and vapor into and out of the volume, as well as the change of storage within the atmospheric volume, this yielding a measure of exchange of water at the earth's surface. This exchange accumulated over the winter season then will be used to determine a relationship with annual runoff (R_e), assuming the change of storage in the terrestrial branch is known.

2. Procedures

Rasmussen (1968) gives, in detail, the computational procedures used in computing the atmospheric water balance. The following sketch of procedures is not meant to provide elaborate instruction, rather it is merely inserted for completeness.

The basic data input is the standard rawinsonde network data taken twice daily at 0000Z and 1200Z (0500 and 1700 MST) over the network shown as open circles in Figure 2. These data (humidity, temperature and wind) were evaluated at 50 mb increments and interpolated to the nine-point boundary grid shown in Figure 2. Grid point 10, the interior point, is the location of the Grand Junction rawinsonde also. We wish to use these data in the estimation of the right-hand side of equation I.1.2. No contribution due to water or ice terms in I.1.2 can be systematically estimated. Rasmussen (1970a) provides an argument demonstrating that these terms are small compared to the water vapor terms. Following that argument I.1.2 may be written.

$$P - E = \underbrace{-\frac{1}{g} \iint \frac{\partial}{\partial t} q dA dp}_{S_a} - \underbrace{\frac{1}{g} \iint C_n q d\ell dp}_{R_a} \quad \text{I.2.1}$$

where g is the acceleration of gravity, t is time, q is specific humidity,

A is surface area, p is pressure, C_n is the component of the horizontal wind normal to the boundary and counted positive outward, $d\ell$ is a horizontal line element on the boundary.

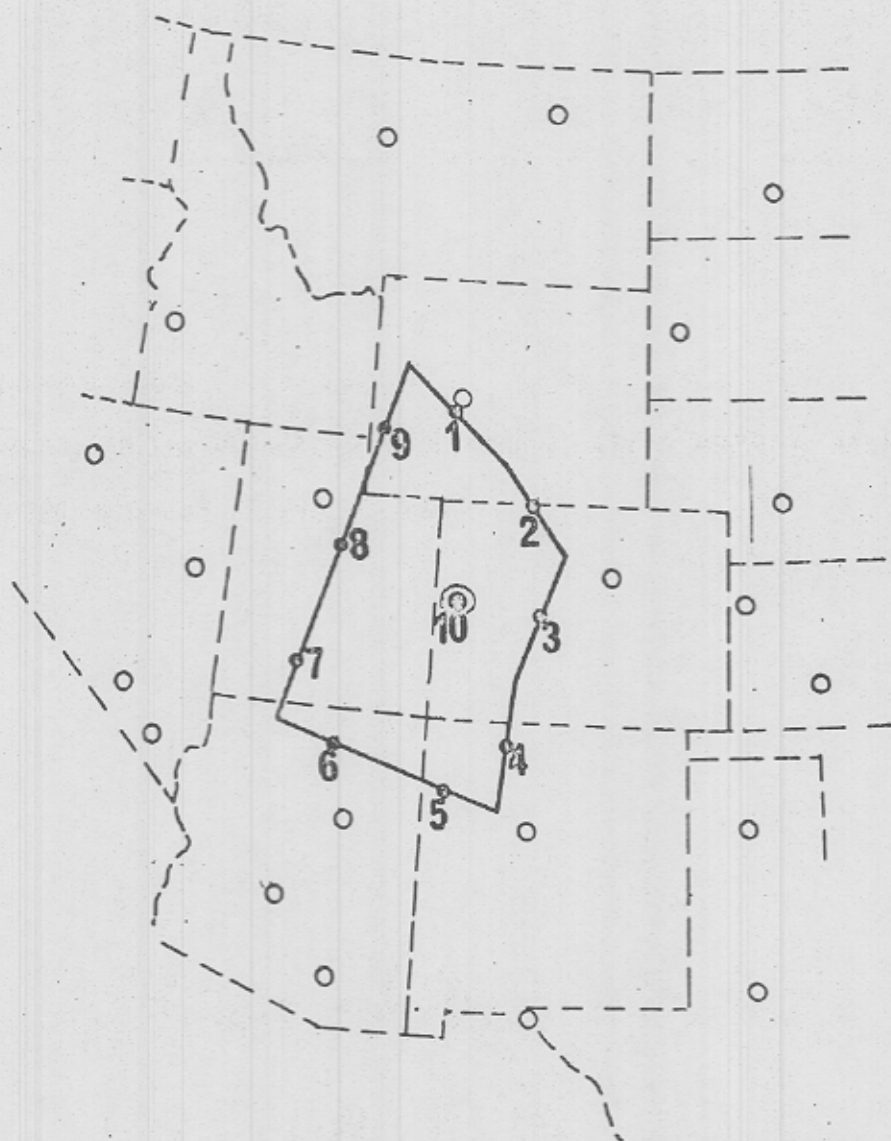


Figure 2. Ten-point grid used in the study, (solid dots). Open circles are locations of rawinsonde stations.

The evaluation of the integrals in I.2.1 done using the 9 point grid of Figure 2, follows the following computational form:

$$P - E = - \underbrace{\frac{1}{g} \frac{\Delta}{\Delta t} \sum_{j=1}^7 \sum_{i=1}^{10} q_{ij} \Delta A_{ij} \Delta P_{ij}}_{S_a} - \underbrace{\frac{1}{g} \sum_{j=1}^7 \sum_{i=1}^9 C_{nij} q_{ij} \Delta x_{ij} \Delta P_{ij}}_{R_a} \quad \text{I.2.2}$$

where the index j refers to the seven possible vertical stratifications and the index i refers to the grid points numbered as in Figure 2. Again, the reader is referred to the article by Rasmussen (1970a) for further discussion.

The evaluation of $P - E$ was done on a daily basis where two computations of the integral R_a were averaged to provide daily estimate. The term S_a is only important in cases where a relatively short time is involved in the computation. Over a longer period of time the time difference of the integral is indeed small compared to R_a and this term need not be evaluated. These daily values then were accumulated over the winter season and a seasonal value of $P - E$ was determined.

Runoff data from the Upper Colorado Basin has historically been referenced at the gauging station at Lee's Ferry, Arizona (e.g. Yevjevich, 1961). With the construction of Lake Powell upstream from Lee's Ferry, the flow of the Colorado has been remaining constant around 8 million acre feet per year. In order to obtain an estimate of the undisturbed flow sum of the flows at Green River on the Green River, Cisco on the Colorado River and Bluff on the San Juan River (this sum denoted by R_e^*), were regressed against the flow at Lee's Ferry. The following equation describes the regression.

$$R_e (\text{Lee's Ferry}) = 1.07 R_e^* - .24.$$

A correlation coefficient $r = .95$ between R_e and R_e^* was obtained.

3. Results

Table I. gives the results of the experiment over the winter seasons, 1957 through 1969. The Year indicates the year in which the season ends, for example, 1957 refers to November, 1956 through April, 1957.

Table I: Compilation of Results, Water Balance Computation and Runoff.

<u>Year</u>	<u>P - E (cm)</u>	<u>R_e (cm)</u>
1957	27.5	8.8
1958	17.3	5.5
1959	19.2	3.5
1960	22.2	4.0
1961	20.0	3.9
1962	22.6	5.9
1963	16.5	0.8
1964	18.0	3.6
1965	26.8	7.7
1966	23.5	3.6
1967	25.5	4.2
1968	31.0	5.4
1969	15.6	5.8

Figure 3. shows seasonal P - E plotted against annual runoff. The points representing the years through 1963 are plotted as dots and one notices a dramatic change in the quality of result prior to and following 1964. The correlation coefficient between P - E and R_e for the period 1957-1963 is $r = 0.34$. The correlation coefficient for the entire period is $r = 0.54$. After running numerous tests on the computation including investigating

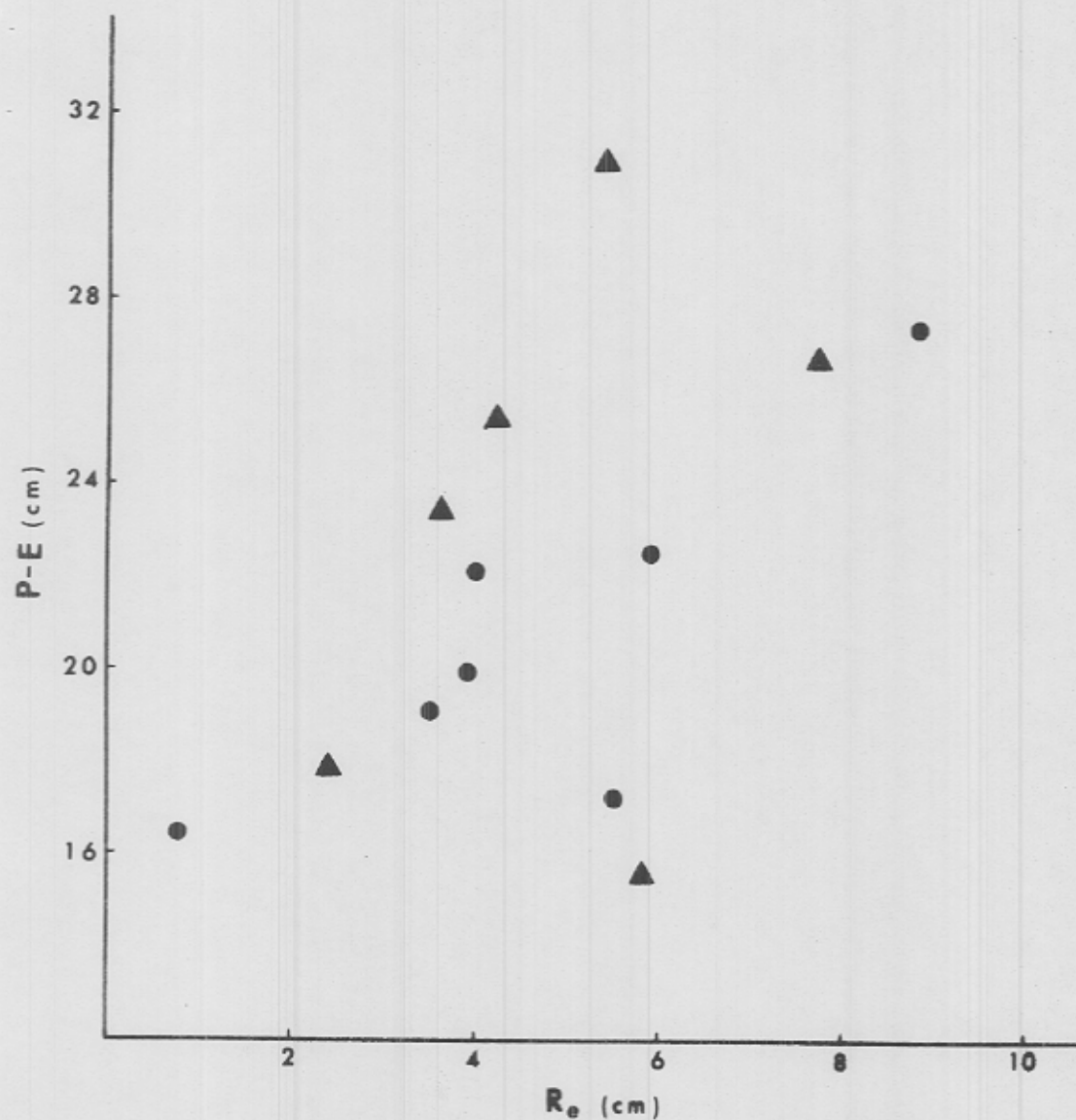


Figure 3. Seasonal (Nov. to April) P - E plotted against Annual (April-March) runoff. Dots denote computations for 1957-1963. Triangles denote computations for 1964-1969.

individual computations including comparison of 0000Z and 1200Z computations, no explanation could be offered for this seeming discontinuity in result. Recent concern with the humidity sensor that was put into operational use in 1964 has been articulated in the literature (e.g. Morrissey and Brousaides, 1970; Tewels, 1970). This source of systematic error, largely unidentifiable in individual soundings, could be dominant in the calculation divergence of water vapor flux as done in equation I.2.2. Errors of the type referred to above can be corrected in the original sounding if the radiation loading and effects of sensor ventilation are known. No tests to date on historical data have been done, but it is apparent that until further research is done, computations of the type attempted here are not worthwhile.

4. Conclusions and Recommendations

The initial test of data over the years of record 1957-1963 provides some element of hope that the atmospheric water balance technique could be a useful tool in the estimation of $P - E$ over large mountainous areas. However, further computations over years of record beyond 1964-1969 suggest that the computation is insensitive when compared to the annual runoff. The relationship that exists between the $P - E$ computed and the R_o realized cannot be used for forecast purposes. It is suggested that the paradox is rooted in errors of humidity measurement associated with a change in instrument instituted in 1964. Further research should center on two central themes.

- 1) The study of the error sources of past data and engineering corrections applied where possible.

2) Renewed effort to calibrate with like standards, on an international as well as national basis, all meteorological sensors. Particular emphasis must be placed upon the measurement of humidity.

Bibliography PART I

- LaRue, J.A., and R.J. Younkin, 1963: Large-scale precipitation volumes, gradients, and distribution. Monthly Weather Review, 91, 393-401.
- McDonald, J.E., 1960: Variability factors in mountain-watershed hydrometeorology in an arid region. Journal of the Arizona Academy of Science, 1, 89-98.
- Morrissey, J.F. and F.J. Brousaides, 1970: Temperature induced errors in the ML-476 humidity data. J. Appl. Meteor., 9, 805-808.
- Palmen, E., 1967: Evaluation of atmospheric moisture transport for hydrological purposes. Report No. 1, World Meteorological Organization/International Hydrological Decade Projects, Geneva, 63 pp.
- Rasmussen, J.L., 1968: Atmospheric water balance of the Upper Colorado River Basin. Atmospheric Science Paper No. 121, Department of Atmospheric Science, Colorado State University, Fort Collins, 112 pp.
- Rasmussen, J.L., 1970a: Atmospheric water balance and hydrology of the Upper Colorado River Basin, Water Resources Research, 6, 1, 62-76.
- Rasmussen, J.L., 1970b: The atmospheric water balance and hydrology of large river basins, Water Resources Bulletin, 6, 4, 631-639.
- Teweles, S., 1970: A spurious diurnal variation in radiosonde humidity records, Bulletin of the American Meteorological Society, 51, 9, 836-840.
- Weiss, L.L. and W.T. Wilson, 1958: Precipitation gauge shields. Transactions, International Association of Scientific Hydrology, Toronto, 1957, Vol. 1, 462-484.
- Yevjevich, V.M., 1961: Some general aspects of fluctuations of annual runoff in the upper Colorado River Basin. Civil Engineering Research Report, CER61VMY54, Colorado State University, 48 pp.

PART II

Atmospheric Water Balance and Precipitation Regimes of Extratropical Cyclones

1. Introduction

The study of the atmospheric water balance of the Upper Colorado River has shown that the dominant factor in the seasonal water budget is the occurrence or non-occurrence of large precipitation events (Rasmussen, 1970; Marlatt and Riehl, 1963). This feature of the annual precipitation regime is not confined to the Colorado Basin alone, similar results are observed over the rest of the Western U.S., as well (Rasmussen, Bertolin and Almeyda, 1971). Invariably, these large precipitation events are produced by large, synoptic-scale, cyclones. It is presumed that the errors in the humidity sensors referred to in Part I, above, would be minimal in the application of such data to these studies since the meteorological conditions of overcast skies, strong gradients of humidity and temperature and strong divergence fields are the rule in these storm systems.

The objective of this paper is to report results of synoptic-scale analyses of the precipitation process of extratropical cyclones. Motivation for this work is derived from the importance of the cyclone in the hydrometeorological setting of the problem of water resources. We wish to present this material as a step in the understanding of the synoptic-scale precipitation processes leading toward a more complete base of knowledge upon which we may understand the systems which we attempt to modify through cloud seeding. Specifically we wish to show:

1. The precipitation pattern with respect to the moving storm system;

2. The transport of water vapor in the atmosphere resulting in the observed precipitation; and
3. The determination of the rate of condensate formation and calculation of the efficiency of the cloud system.

The following discussion is based upon the study of two storm systems that traversed North America in February, 1961 and January, 1967. The 1961 case was an "average system yielding precipitation over a wide area but with no conspicuously large local accumulations. The 1967 storm system, on the other hand, was characterized by a band of heavy precipitation stretching from Michigan southwestward to Eastern Kansas. (Figure 1) This storm has been known as the "great Chicago snowstorm of 1967" (Smith, 1967). A fourth objective of this paper is to sketch out an idea we propose as a mechanism for this locally heavy precipitation anomaly.

2. Analysis

Our method of analysis is based upon superimposing a rectangular grid system centered on the moving surface low pressure center (grid area $6^{\circ} \times 8^{\circ}$ latitude in the 1961 case and $8^{\circ} \times 12^{\circ}$ latitude in the 1967 case). (Figure 1) All our results then must be interpreted as being relative to the moving storm system. Figures 2a and 2b show the path of the cyclone centers as the storms traverse the continent. The dots and circles denote the locations of the hourly precipitation gauge data used in the analysis. We determined the precipitation relative to the moving storm center through the following analysis procedure.

1. The hourly increments of the path of all the gauges were determined and the hourly precipitation noted for each increment (Figure 2c).

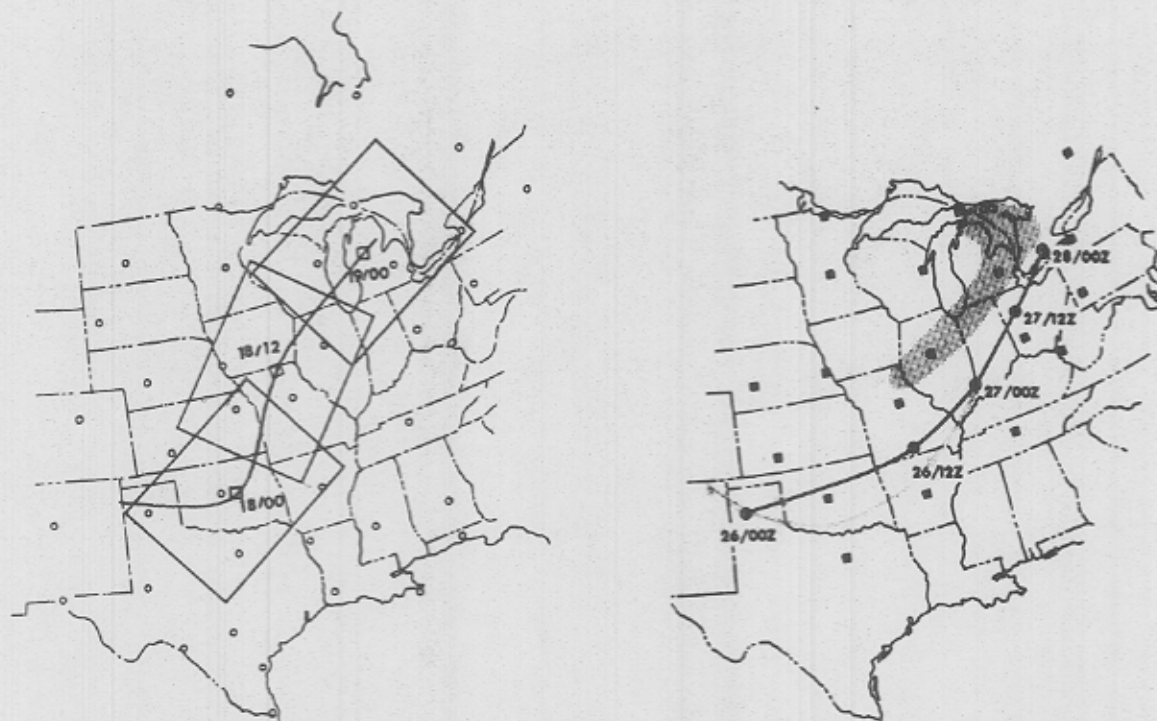


Figure 1 Left: Storm track and grid locations for 1961 case. Right: Storm track and precipitation belt (snow depth greater than 10 inches) for 1967 case. Open circles on the left and squares on the right denote locations of rawinsonde stations.

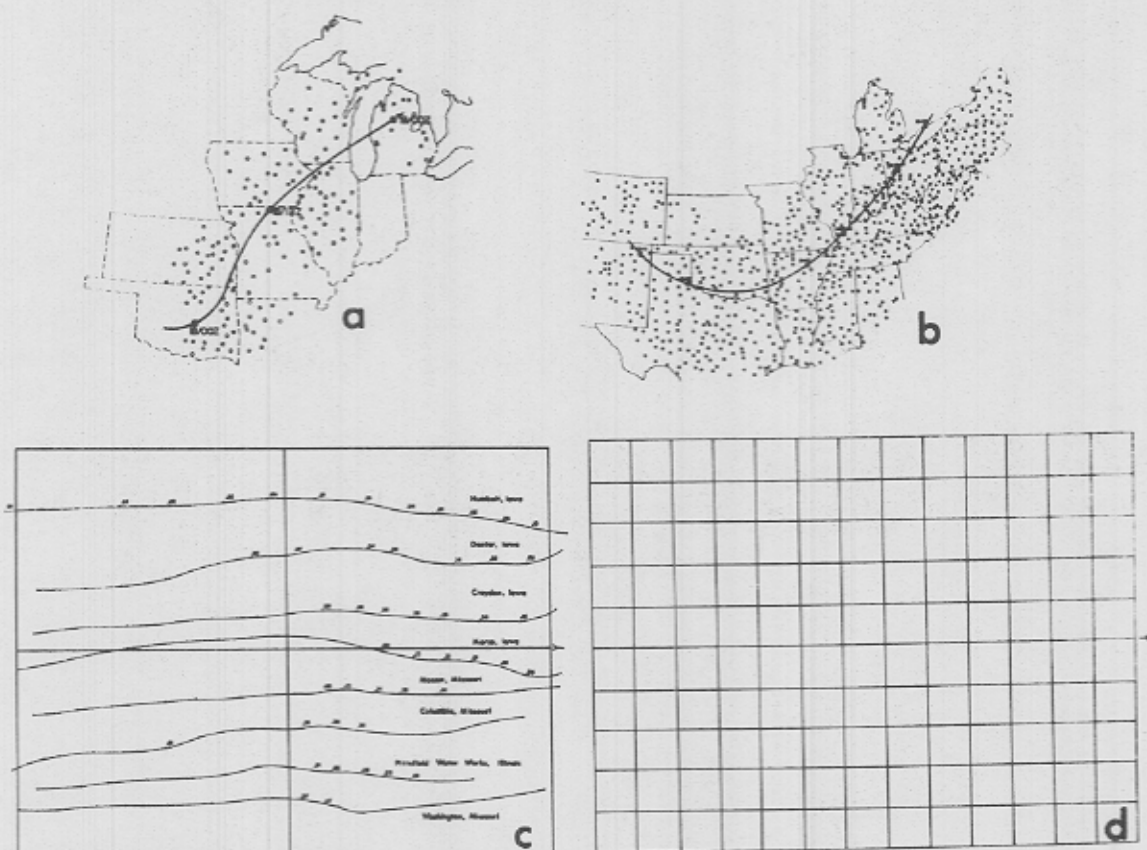


Figure 2 a. and b.: Storm tracks and hourly precipitation stations used in the analysis. c.: Typical station paths through the grid area with hourly values entered. d.: Area averaging grid.

2. After all the data were accumulated for all possible stations during the period ± 3 hours from the 0000Z and 1200Z map times, average quantities were calculated for each box of the grid shown in Figure 2d.
3. These 130 average values were analyzed yielding the precipitation maps shown in Figures 3 and 4.

Note that the precipitation maximum relative to the storm center, in both cases, moves across the grid with time. This reflects the movement of the frontal systems as the storm occludes in the 1961 case and reflects some unusual features of the low level wind field in the 1967 case. We will discuss this problem in the last section of this paper. The local intensities of precipitation and area averaged precipitation are surprisingly uniform for the two storms. The area average precipitation for each analysis period is presented in Table I.

Atmospheric water balance: We computed the atmospheric water budget of these two systems, our objective was to study the divergence of flux of water vapor through the atmospheric volume over the rectangular grid. We wished to determine the quantity precipitation minus evaporation as a residual and compare this quantity to the gauge precipitation, assuming the evaporation to be small.

The atmospheric water balance may be written (e.g. Palmén, 1967; Rasmussen et al., 1969):

$$P - E = - \frac{\partial}{\partial t} \int q \rho \delta V - \int C_{nr} q \rho \delta \sigma \quad \text{II.2.1}$$



Figure 3. Precipitation pattern for 1961 case (inches per hour).
 a. 18 February 0000Z. b. 18 February 1200A.
 c. 19 February 0000Z.

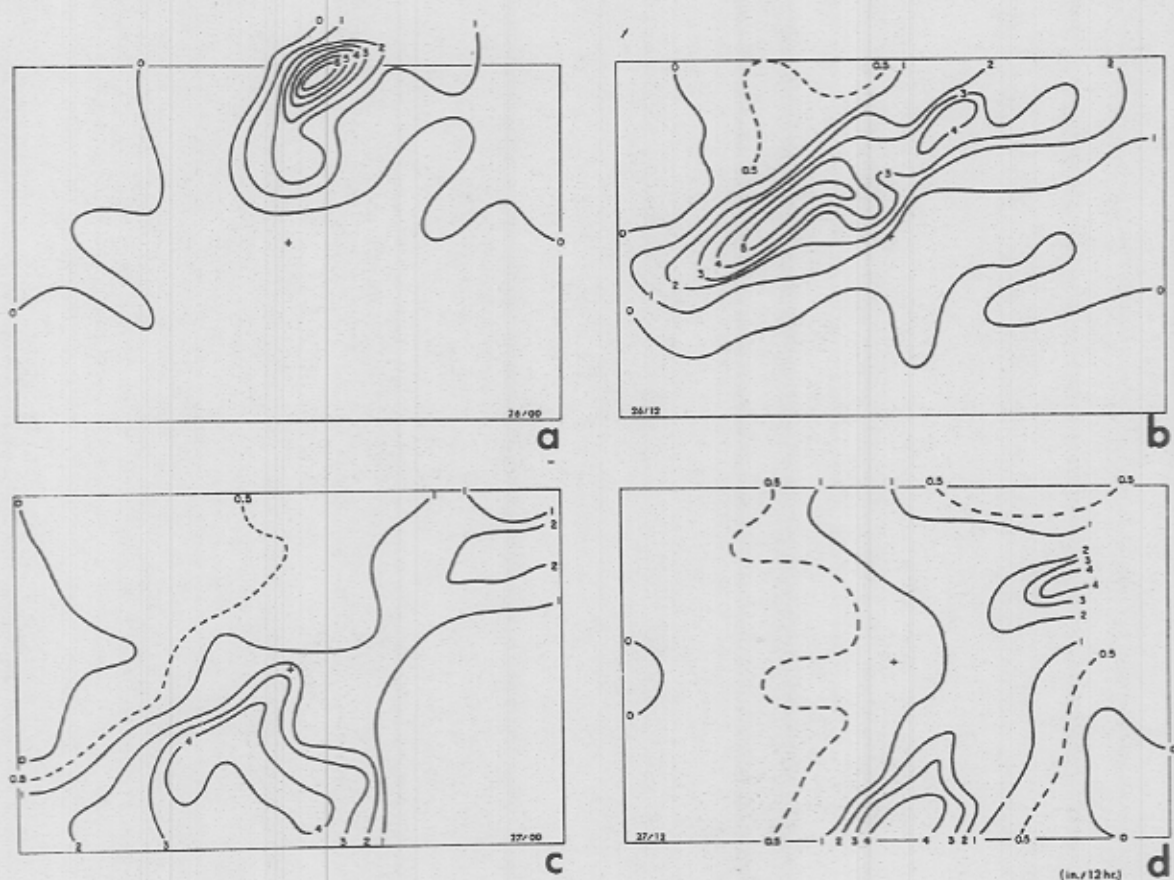


Figure 4. Precipitation pattern for 1967 case (inches per 12 hours).
 a. 26 January 0000Z. b. 26 January 1200Z.
 c. 27 January 0000Z. d. 27 January 1200Z.

where: ρ = density of air V = volume
 P = precipitation rate C_n = wind component relative to the
 E = evaporation rate moving storm normal to vertical
 q = specific humidity boundary, positive outward
 σ = surface area of vertical wall of
volume.

This equation was evaluated over the grid shown in Figure 5 for 50 mb steps in the vertical up to 200 mb. The correlation term ($C_n q$) was

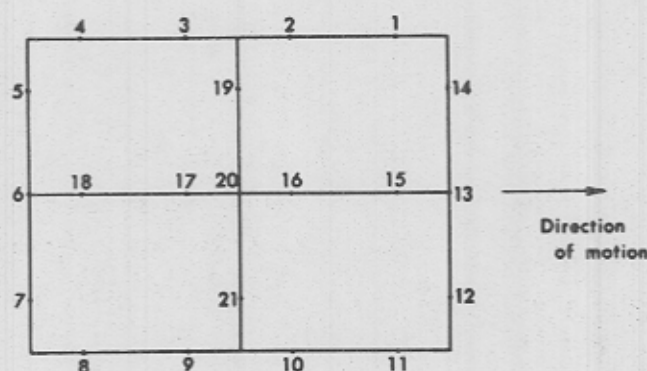


Figure 5. Grid over which the evaluation of equation was accomplished. Central point (no. 20) in storm center location.

broken into mean (ageostrophic) and deviation (eddy) components in the finite difference formulation (see Rasmussen et al., 1969).

$$P - E = \frac{\Delta}{\Delta t} \sum_{j=sfc}^{top} A_j q_j \frac{\Delta p_j}{g} - \sum_{j=sfc}^{top} l_j (\overline{C_n q})_j \frac{\Delta p_j}{g} - \sum_{j=sfc}^{top} l_j (\overline{C'_n q'})_j \frac{\Delta p_j}{g} \quad \text{II.2.2}$$

where: p = pressure
 l = distance on boundary
 A = area on pressure surface
 \wedge = area average
 $-$ = boundary average
 $'$ = boundary deviation from average.

Each of the terms of equation II.2.2 contributes significantly to the water budget of the cyclone. Figure 6 shows the time rate of change of precipitable water in the 1967 case; the rate of change over 12 hours approaches the yield of the system. The 1961 case exhibits a similar profile with time and the maximum denotes the time with the largest volume

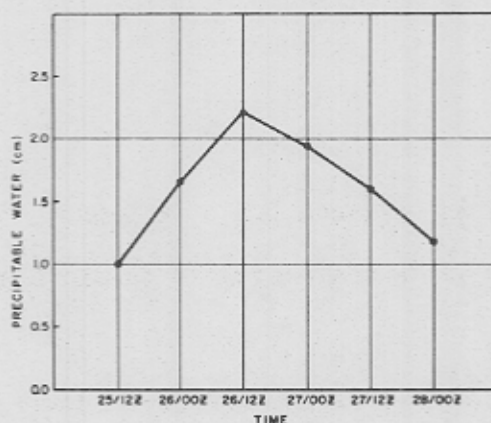


Figure 6. Variation in time of the water vapor stored in the atmospheric volume. Units are equivalent depth of water evenly distributed over the area, precipitable water.

of maritime air in the system. Figure 7 shows the vertical section of the mean and eddy divergence of flux terms. The mean terms are dominant in the lower levels showing the importance of the ageostrophic wind field. Aloft the eddy term often is positive in contribution showing a correlation between outflow and moist air in conjunction with inflow and dry air.

Vertical integration of the terms results in the values shown in Table I.

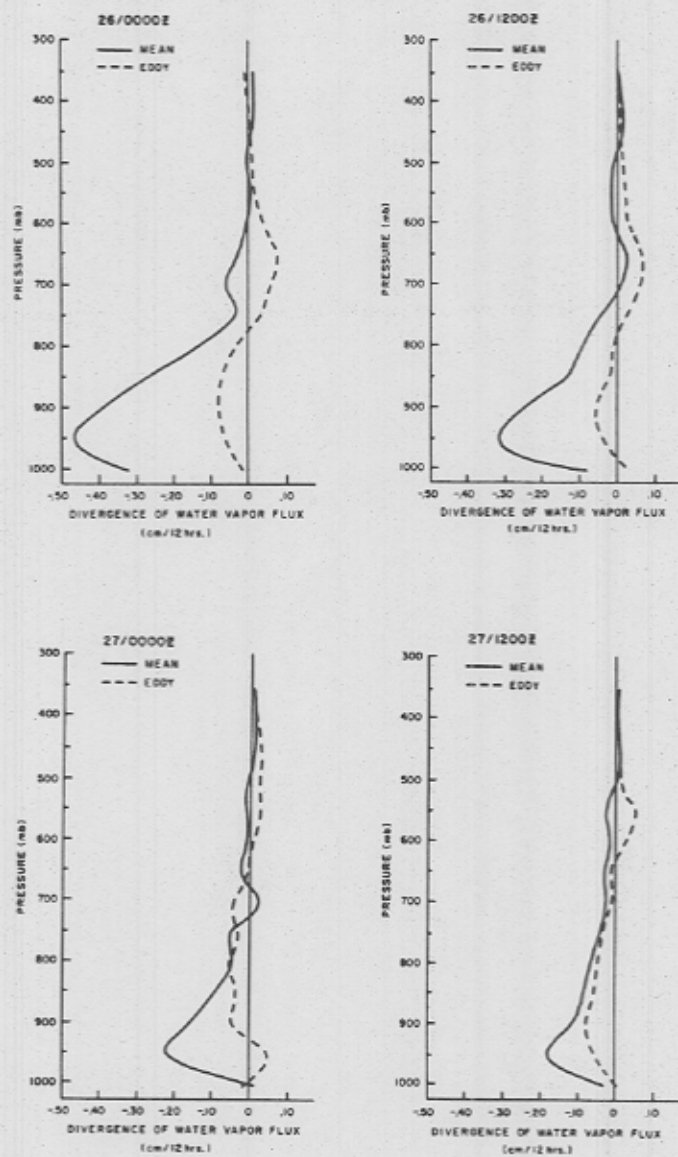
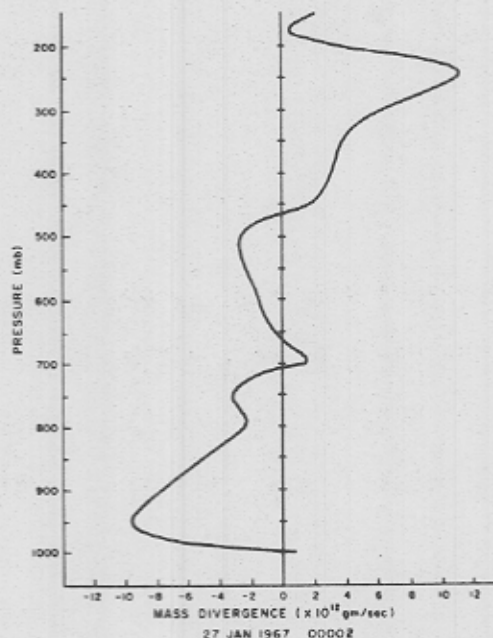


Figure 7. Vertical profiles of the mean and eddy components of the divergence of water vapor flux.

Condensate computation: The structure of the storm, showing a source of water from the strong ageostrophic wind field near the surface and the fact that for the total atmospheric volume the computation of mass flow shows that mass-balance was attained (Figure 8.), lead us to attempt to

Figure 8: Vertical profile of mass divergence in the atmospheric volume.



calculate the rate condensate formation by determining the mass ascent of various thermodynamically homogenous sections of the storm. Our analysis is based upon the assumption that the air conserves its equivalent potential temperature: (Rasmussen, et al., 1969).

$$\theta_e = \theta_d \exp \frac{Lq}{C_p T_s} \quad \text{II.2.3}$$

where: θ_d = dry potential temperature C_p = specific heat at constant pressure and
 L = latent heat of vaporization T = temperature of the air parcel at saturation

The analysis follows the following procedure:

1. Each grid point has a rate of mass inflow or outflow of a certain Θ_e . We group these Θ_e values into groups of 5°C range and proceed to determine the vertical mass flows for each group. The accumulation is initiated from the bottom.
2. Having the vertical mass flows then and knowing the initial conditions, the air is followed to saturation from where the condensate is calculated from the change of saturation specific humidity following the rising cloud mass in constant Θ_e process.
3. The condensate is accumulated over all ascending masses to yield the values representative of the storm.

Table I also lists the results of the condensation rate computation. On the average this rate of condensate leads to storm efficiencies of 0.90, where efficiency is defined as the ratio precipitate to condensate. One may interpret this to be quite high in light of other estimates of cloud efficiency, for example of orographic clouds which have efficiencies on the order of 0.20.

Figure 9 shows the distribution of condensate formed as a function of temperature. As one might expect in storms with the mass flow characteristics of these cases the predominate condensate formation is at a surprisingly warm temperature. Note as the storm matures the shift is toward a more uniform distribution of condensate formation with temperature. Figure 10 is the composite condensate picture of all time periods of both storms. Since cloud seeding affects the growth characteristics of droplets

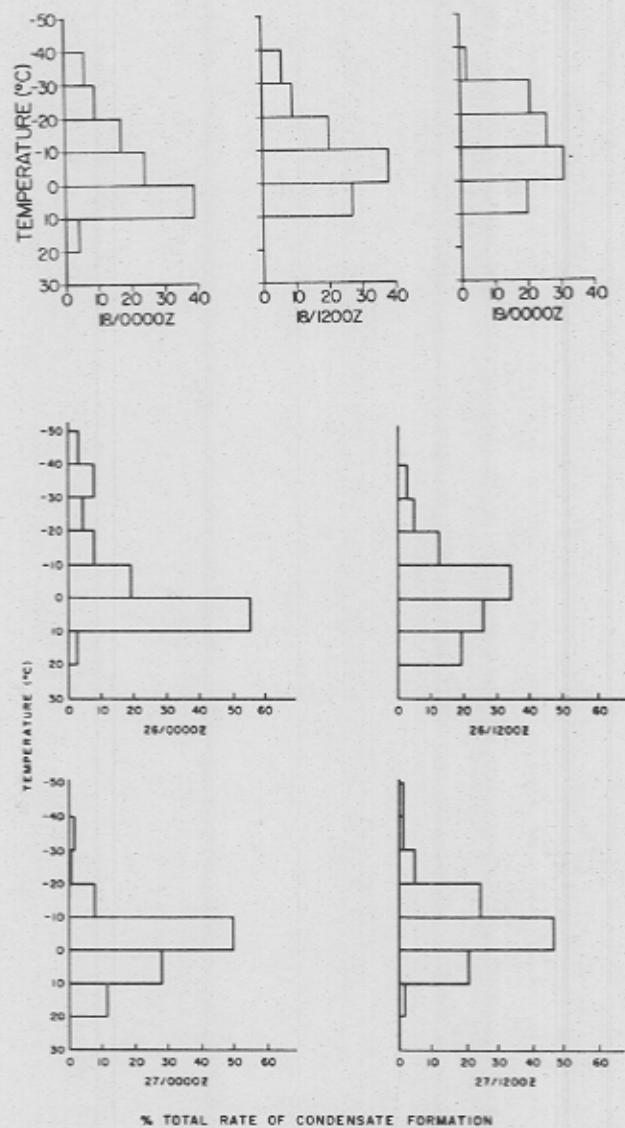


Figure 9. Distribution of condensate formed as a function of cloud temperature. Top: 1961 case. Bottom: 1967 case.

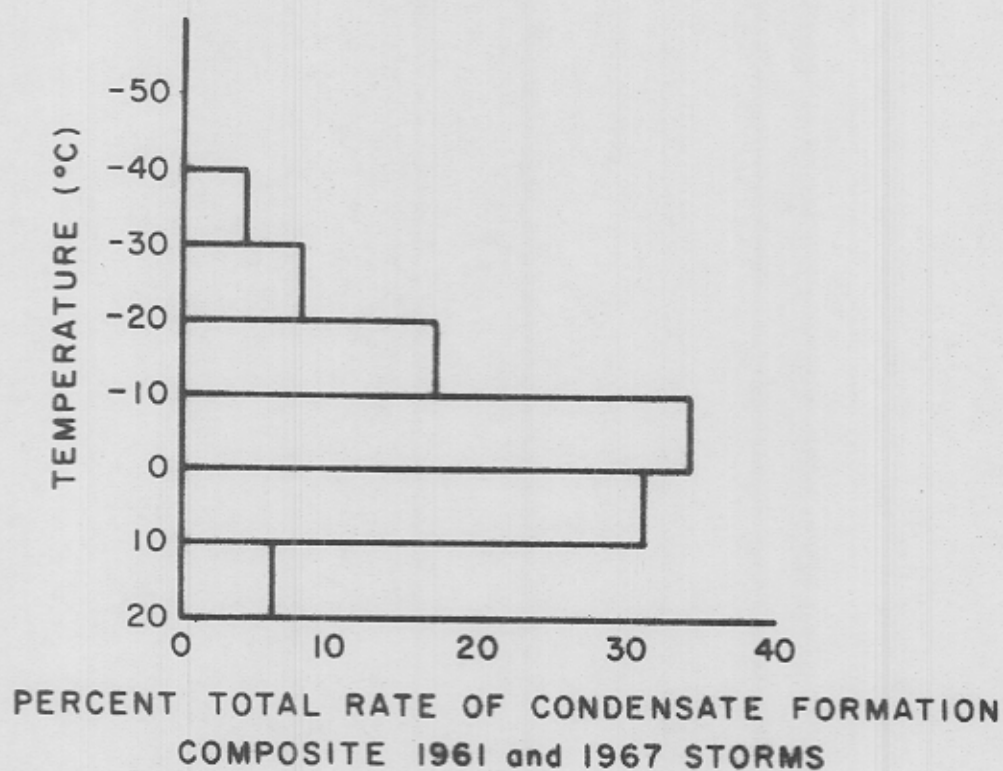


Figure 10. Distribution of condensate formed as a function of cloud temperature. Composite of all time periods.

at relative warm temperatures the forcing of cloud seeding on storm systems with this condensate profile could be dramatic.

The snow belt -- January 1967 storm: It is of interest to investigate further the unusually heavy precipitation band extending from northeast Michigan southwestward into Missouri. (see Figure 1.) We will briefly sketch a proposed mechanism producing this anomaly. A more detailed analysis will soon be published (Rasmussen and Hadley, unpubl. manus.). Figures 11, 12, 13 show that the intensity of precipitation within the band (Figure 12) was much more intense than outside the band (Figures 11 and 13). Inspection of low level charts (900 - 800 mb) showed that there existed a localized zone of strong wind speed to the north of the center. Constructing equivalent potential temperature surfaces and determination of air parcel trajectories demonstrated that in the first approximation one may use the concept of potential vorticity,

$$\frac{d}{dt} \zeta_a \frac{\partial \theta}{\partial p} = 0$$

to demonstrate that as the parcel moves toward greater values of ζ , $\frac{\partial \theta}{\partial p}$ must decrease leading toward conditional instability and convection (Figure 16), (Hadley, 1970). This pattern rotates relative to the moving system such that it is located over one area for up to 30 hours yielding extreme local precipitation amounts.

3. Conclusions: We have shown that the precipitation pattern relative to a moving storm system is highly banded and moves relative to the moving

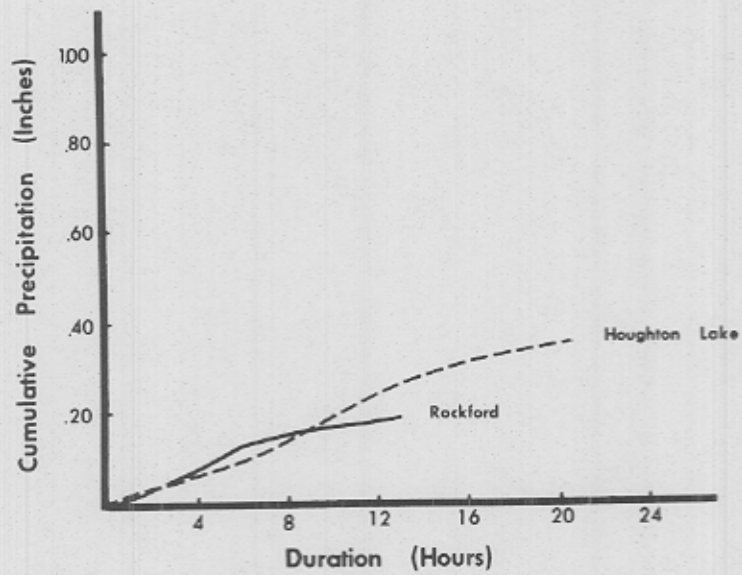


Figure 11. Cumulative precipitation for 1967 case for stations just north of the heavy precipitation belt.

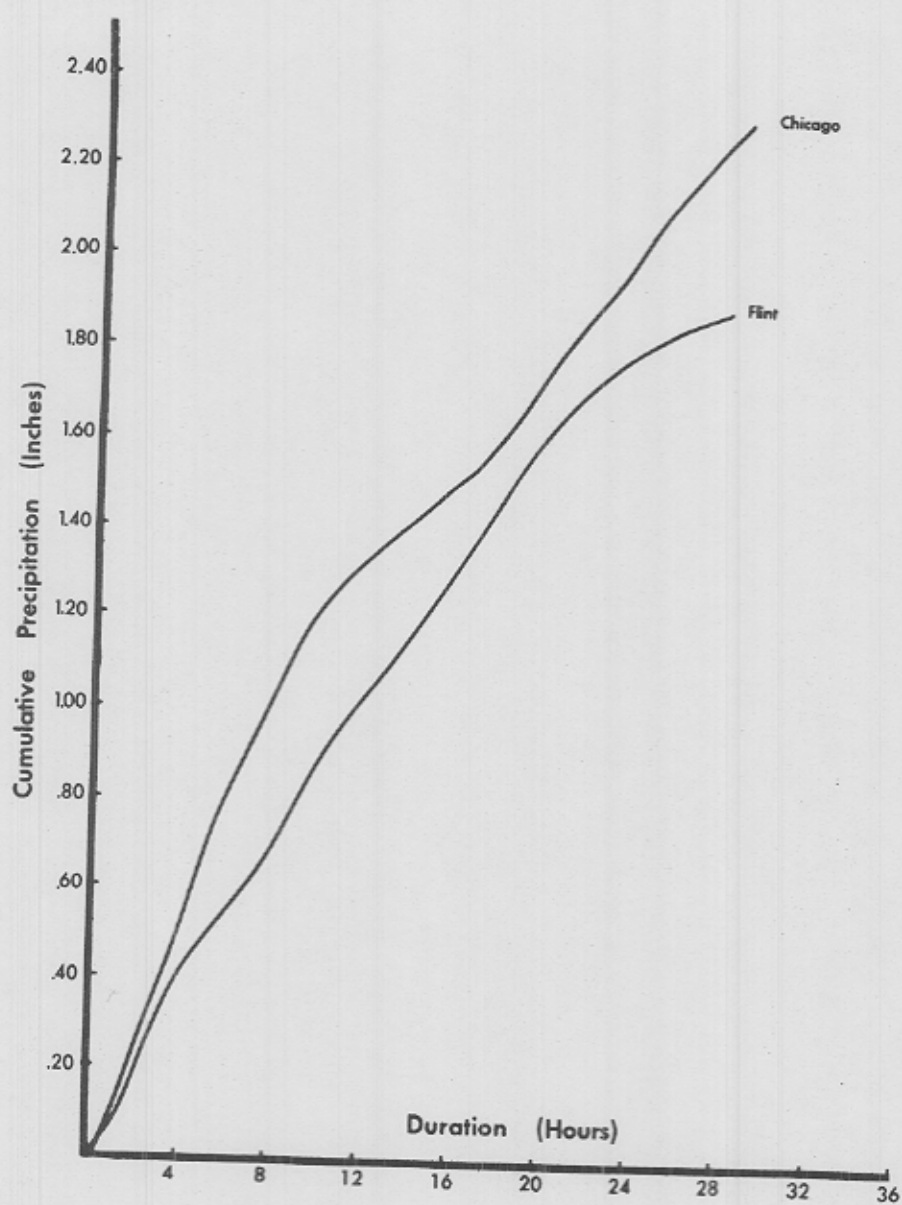


Figure 12. Cumulative precipitation for 1967 case for stations within the heavy precipitation belt.

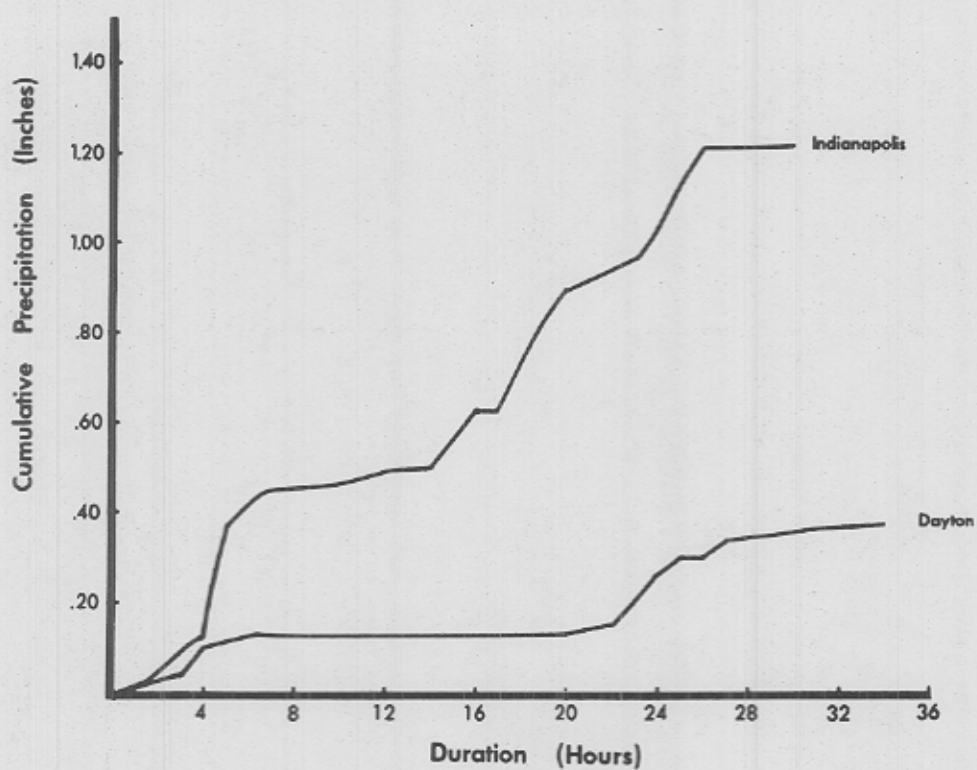
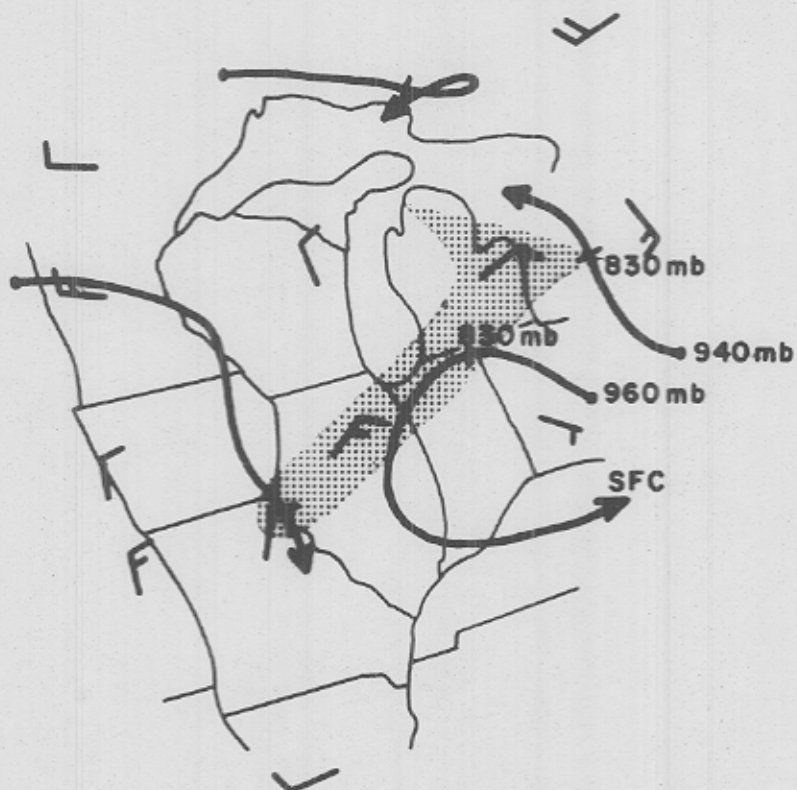


Figure 13. Cumulative precipitation for 1967 case for stations south of the heavy precipitation belt.

coordinate. The areal average yield is similar for both a very heavy local snow producing system and an average snow producing system. The inflow of vapor is accomplished by the ageostrophic component of the wind field and the atmospheric water balance provides a good estimate of the observed precipitation. The precipitate to condensate ratio is 0.90. The condensate largely forms at a temperature warmer than -10°C . The mechanism for the generation of locally intense snow fall in the 1967 case is proposed as being caused by the dynamic effect of a low level wind field initiating convective activity by stretching of the air column and the advection into more positive vorticity field.

Further application of the atmospheric water balance technique appears to be most beneficial in the diagnostic studies of vigorous circulation systems like the extratropical cyclone. Questions with regard to the forcing of the system by cloud modification are questions that must be faced in order to approach the plan of water resource management from the position of knowledge.



TRAJECTORIES ON 300°K θ_e SURFACE
 26/1200Z - 27/1200Z JAN. 1967
 WIND RECORD IS FOR 27/0000Z

Figure 14. 24-Hour trajectories of air parcels on the 300°K θ_e surface. 26/1200Z - 27/1200Z. Wind field is for 27/0000Z. Shaded area outlines the belt of heavy snowfall.

Bibliography PART II

- Bradbury, D.L., 1957: Moisture Analysis and Water Budget in Three Different Types of Storms. J. Meteorol., 14:559-565.
- Hadley, D.L., 1970: Precipitation Patterns in a Cyclone. M.S. Thesis, Department of Atmospheric Science, Colorado State University, Fort Collins, Colorado, 40 pp.
- Marlatt, W. and H. Riehl, 1963: Precipitation regimes over the Upper Colorado River. Journal of Geophysical Research, 68, 6447-6458.
- Olascoaga, M.J., 1950: Some Aspects of Argentine Rainfall. Tellus, 2:312-318.
- Palmen, E., 1958: Vertical Circulation and Release of Kinetic Energy during the Development of Hurricane Hazel into an Extratropical Storm. Tellus, 10:1-23.
- Palmen, E., 1967: Evaluation of Atmospheric Moisture Transport for Hydrological Purposes. Report No. 1, WMO, Internat. Hydrolog. Decade Projects, Geneva, 63 pp.
- Palmen, E. and E.O. Holopainen, 1962: Divergence, Vertical Velocity and Conversion between Potential and Kinetic Energy in an Extratropical Disturbance. Geophysica, 8:89-113.
- Petterssen, S., 1956: Weather Analysis and Forecasting, 2nd ed. McGraw-Hill, New York.
- Rasmussen, J.L., 1968: Atmospheric Water Balance of the Upper Colorado River Basin. Atmospheric Science Paper No. 121, Department of Atmospheric Science, Colorado State University, Fort Collins, Colorado, 112 pp.
- Rasmussen, J.L., R.W. Furman, and H. Riehl, 1969: Moisture Analysis of an Extratropical Cyclone. Arch. Meteorol. Geophys. Bioklimatol., Ser. A., 18:275-298.
- Rasmussen, J.L., 1970: Atmospheric Water Balance and Hydrology of the Upper Colorado River Basin, Water Resources Research, 6, 1, 62-76.
- Rasmussen, J.L., G. Bertolin and F.G. Almeyda, 1971: Grassland Climatology, Technical Report to Grasslands Biome, International Biological Program. Natural Resources Ecology Laboratory, Colorado State University, Fort Collins.
- Riehl, H., 1949: Some Aspects of Hawaiian Rainfall. Bull. Amer. Meteorol. Soc., 30:176-188.
- Smith, J.S., 1967: The Great Chicago Snowstorm of '67. Weatherwise, 20(6): 248-253.